

Dynamic Simulation of a Hybrid Solar and Ocean Thermal Energy Conversion System

Mohammad Ali Azghandi¹, Javad Rouhi¹, Roya Ahmadi¹

¹(Department of Electrical, Mazandaran University of Science and Technology, Iran)

ABSTRACT: Ocean thermal energy conversion (OTEC) is a system in which electricity is produced using small temperature difference of warm surface water and deep cold water in oceans. This paper analyzes the dynamic stability and performance simulation results of a solar and ocean thermal energy conversion (SOTEC) system connected to a power grid through undersea cables. In SOTEC, the temperature of warm sea water was boosted by using a typical low-cost solar thermal collector. The complete system model is established from the dynamics of each subsystem and their interconnections. Specifically, we examine stability and performance of the power system against such disturbance conditions as slow variations of solar radiation and severe three-phase short-circuit fault at the power grid. Simulation results indicate that the design of a power system stabilizer can improve the damping of power system under various disturbance conditions.

Keywords -Dynamic stability, power system stabilizer (PSS), renewable energy, solar and ocean thermal energy conversion (SOTEC).

I. INTRODUCTION

Global concerns about damages to the environment, reduction of fossil resources and increasing demand for electrical energy has contributed to the global shift toward developing and using renewable energy. Such concerns have made scientists and politicians to move toward developing such alternative energies which are cost efficient and can replace fossil energy in large scale. Taking into account the existence of large oceans on earth with regular daily thermal differences in surface and deep waters, OTEC can be made into a considerable and reliable source of energy in many coastal regions, from Hawaii, to Puerto Rico, south of Mexico and coastal cities in India and potentially produce electricity requirements in such areas [1]. In such coastal areas as mentioned above the existence of favorable thermal oceanic difference as well as high cost of electricity production from fossil resources makes the use of OTEC a necessity. In addition, there are other advantages to using OTEC, such as producing fresh water and various other nutrients.

In this paper we list a number of studies working on OTEC system and ways to improve solar-concentrated systems. In [2], the simulation and performance evaluation of a pilot OTEC system, using a combination of water and ammonia as working fluid has been proposed. In [3], the authors have examined the effects of temperature as well as flow rate of sea water. In doing so, the authors have taken into accounts such factors as pipe diameter, seawater depth, and seawater flow rate. The authors have investigated the functions of a 50 MW OTEC System with an Offshore Solar Pond (OSP) in [4]. The results of the study indicated that a 3 to 12 percent efficiency improvement will be obtained if an OSP is added to the OTEC system. While the existing OTEC models have a single stage of power cycle, adding an extra stage can improve the obtained power from power cycle as much as 36 percent. Such consecutive stages can amount up to three or even further stages. In doing so, however, a balance must be created between pure power output and costs on the one hand and complexity and increase in size of thermal converters on the other hand. In any case, the amount of costs is a determining and limiting factors against designing multiple-stage programs [5]. Solar pond or solar energy collectors can be used in order to improve the performance of thermodynamic cycle [6]. In [7], the authors assess the dynamic stability of a grid-connected, solar-concentrated ocean thermal energy conversion system (SC-OTEC). This paper presents the normal functions of a grid-connected system as well as its transient response against various disturbances, such as sunshine deviations and short-circuit fault. Combining OTEC system with classic thermal power-plant, we can use the energy obtained from thermal discharge in condenser. Using such energy, both improves the thermal efficiency, and reduces the thermal pollution of the system [8, 9]. Manufacturing and testing mock-up for commercialization of the OTEC (50MW) power plant were presented in [10].

This paper examines and develops a connected OTEC whose thermal efficiency have improved. The model we present in this paper is particularly appropriate for transient simulations of three-phase power system. Based on mathematical models and functions of an OTEC power system, we perform our assessment which is based on thermodynamic principles, heat transfer, and working fluid. Eventually, we obtain the complete model of the system based on the dynamics of each subsystem and its internal interconnection. This paper is organized in five sections. In section II we indicate basic mathematical models used in the system while it is connected to a

power grid through transmission lines. Section III is an illustration of the design procedure of power system stabilizer (PSS). In section IV we present simulation results of a 50 MWe SOTEC system performance against slow variation in solar radiation conditions and three-phase short-circuit fault at power grid. Finally, in section V we conclude summarizing the main points presented in this paper.

II. MATHEMATICAL MODELS OF THE PROPOSED SYSTEM

Fig. 1 indicates a one-line diagram of proposed system connected to the grid. This system is located far from the shore and is connected to a substation by cables.

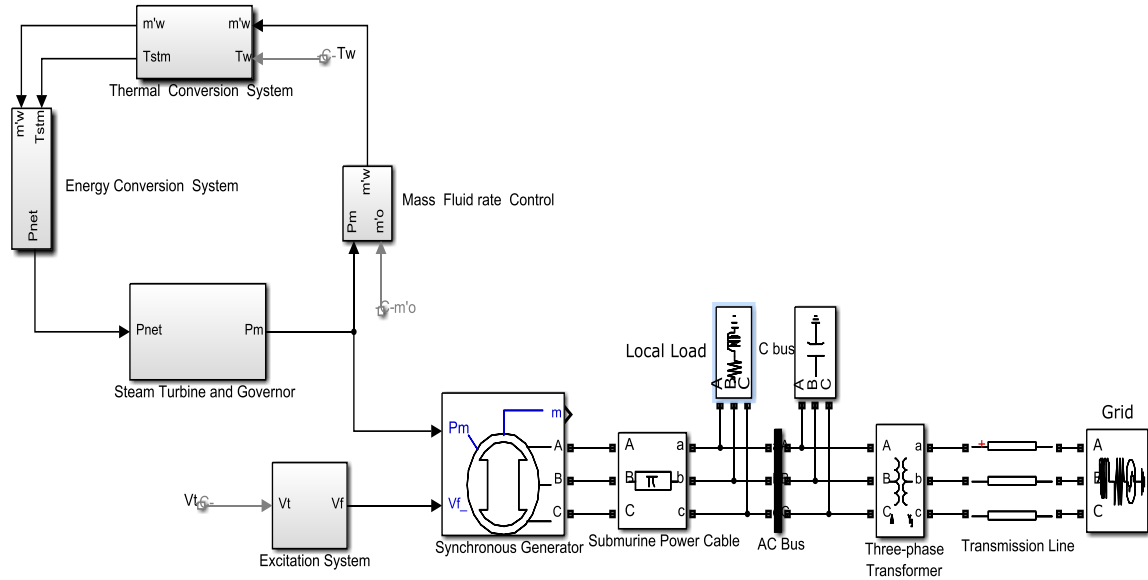


Fig. 1. One-line diagram of the studied grid-connected S-OTEC system.

A. Thermal Conversion System

Heat exchangers must absorb heat and transfer it to surface water. The energy balance equation for heat conversion is indicated below [11],

$$M_w \cdot c_w \cdot \frac{dT_{stm}}{dt} = q_u - U_s \cdot A_s (T_{stm} - T_a) - \dot{m}_w \cdot c_p (T_{stm} - T_w) \quad (1)$$

$$q_u = A_c \cdot F_R [S \cdot \alpha \cdot \tau - U_L (T_{stm} - T_a)] \quad (2)$$

$$F_R = \frac{\dot{m}_{cs} \cdot c_w}{A_c \cdot U_L} [1 - \exp(\frac{-A_c \cdot U_L \cdot F}{\dot{m}_{cs} \cdot c_{cs}})] \quad (3)$$

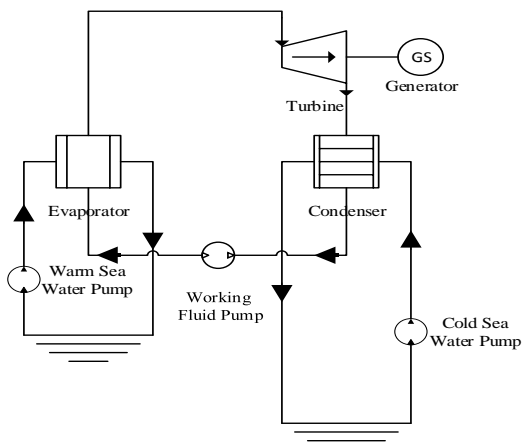


Fig. 2. Block diagram of a closed-cycle OTEC system.

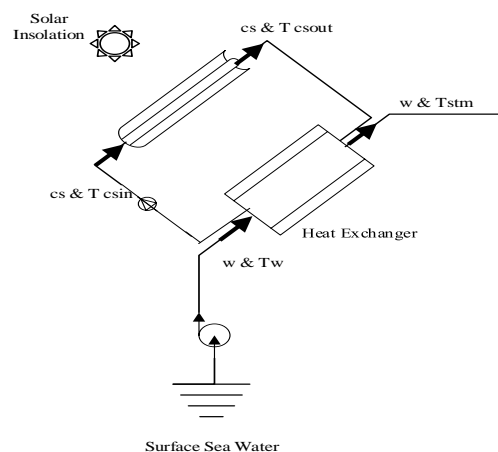


Fig. 3. Framework diagram of the proposed solar concentrated system and the heat exchanger.

In which, M_w (kg) is the fluid mass in the heat exchanger, C_w (J/kg) is the heat capacity of water, T_{stm} ($^{\circ}C$) is the average output temperature of the heat exchanger, q_u (kw) is the heat absorbed by the water in the centralized

pipe, U_s is the dimensionless heat loss coefficient for collector of the heat exchanger, $A_s (m^2)$ is the surface area of the heat exchanger, $T_a (^{\circ}C)$ is the ambient temperature, $\dot{m}_w (kg/s)$ is the surface warm mass flow rate, $c_p (j/kg \cdot ^{\circ}C)$ is the heat capacity of the seawater, and $T_w (^{\circ}C)$ is the temperature of the surface warm seawater. A_c is the aperture area of the parabolic mirror in m^2 , F_R is the dimensionless heat removal factor, S is the solar insolation in w/m^2 , α is the dimensionless absorbance of the absorber pipe, τ is the dimensionless transmittance of the glass cover, U_L is the heat loss coefficient for collector in $w/m^2 \cdot ^{\circ}c$, \dot{m}_{cs} is the water mass flow rate in kg/s , and F' is the dimensionless collector efficiency factor.

B. Energy Conversion System

The following is the energy conversion equation in this study. There are two inputs in this equation; the surface seawater mass fluid rate (\dot{m}_w) and the average output temperature of the heat exchanger (T_{stm}) [12, 13].

$$P_{net} = \frac{\dot{m}_w \cdot c_p \cdot \rho \cdot 3\eta}{16(1+\eta)(T_{stm} + 273.15)} [(T_{stm} - T_c)^2 - 0.3 (\Delta T_{design})^2] \quad (4)$$

In this equation $P_{net} (W)$ is the net power, $\rho (kg/m^3)$ is the average density of seawater, η is the ratio of the cold-seawater flow rate to the warm-seawater flow rate in the process, $T_c (^{\circ}C)$ is the temperature of the depth cold seawater, and ΔT_{design} is the ideal design temperature difference. It should be mentioned, however, that total loss of pumps in the energy conversion system is usually estimated and calculated in the above formula.

C. Turbine- Governor Model, SG, Excitation System and Other

In this study, the characteristics of turbine are determined by the kind of working fluid used with low-pressure ratios and relatively high mass flow [14].

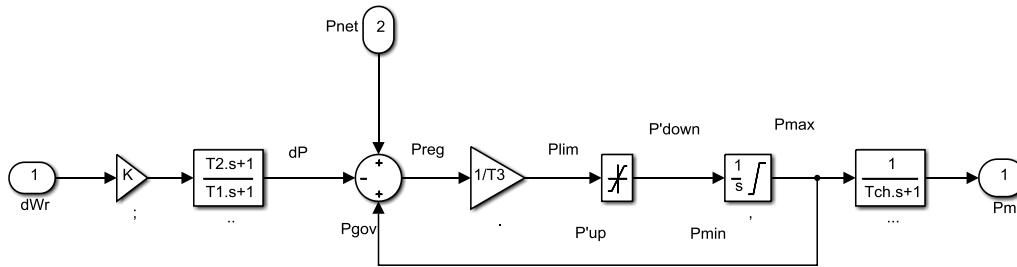


Fig. 4. Block diagram of the used governor and turbine.

To read further about the pu d-q axis equivalent-circuit model of the studied SG and equivalent circuit models from the output terminal of the SG to the power grid refer to references [15, 16].

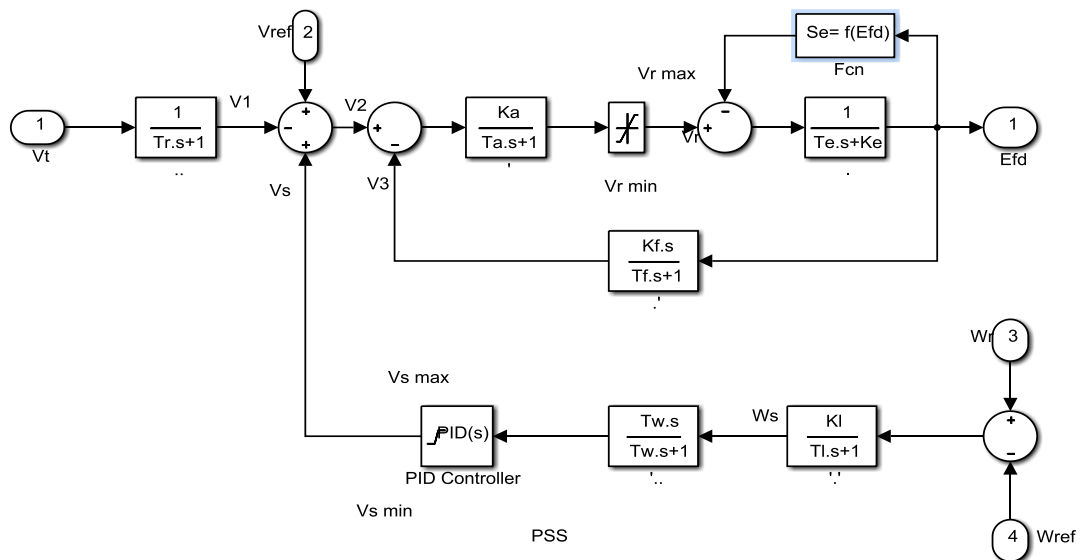


Fig. 5. Block diagram of the excitation system including the PID PSS.

III. DESIGNING PID PSS

The main role of a stabilizer in a power grid is to add damping to the generator rotor oscillation by controlling its excitation using auxiliary stabilizing signal(s). To provide damping, stabilizer must create an

electrical torque component in phase with rotor speed deviations. Often it is necessary for stabilizer to play a role in a range of frequencies, rather than a single frequency. The phase characteristic that must be compensated will change as system conditions change. Thus reconciliation is achieved and a single characteristic has been chosen for various system conditions. First, non-linear system equations must be developed and linearized around nominal operating point. This is done in order to attain a set of linearized system dynamic equations.

$$\dot{X} = AX + BU + VW \tag{5}$$

$$Y = CX + DU \tag{6}$$

In this equation X is the state vector, Y is the output vector, U is the external or compensated input vector, and W is the disturbance input vector. Also in this equation A, B, C, and D are all constant matrices with varying dimensions.

In the design of current PID PSS, The variation term W and external input U have been ignored through considering the equation as $D = V = 0$. There are three sub state vectors into which that vector X can be appropriately positioned; electrical system, mechanical system, and SOTEC System. In Fig. 6 and Fig.7 eigenvalues of the system without PID PSS and with PID PSS have been indicated respectively. Accordingly, system stabilizer has been designed by Matlab through optimization method for obtaining appropriate damping. Since most associated system values are fixed on the complex plane, only the exciter mode and electromechanical mode have been indicated in table 1, that are located close to the imaginary axis of the complex plane [17]. Results indicate that although the designed PID PSS increases damping of mechanical mode (resulted from turbine-governor system) significantly, it slightly decreases electrical mode damping (resulted from excitation system).

TABLE I
EIGENVALUES OF THE STUDIED SYSTEM UNDER VALUES OF $V_t = 1\text{pu}$ AND $P_g = 0.8\text{pu}$

Without PSS	Position (rad/s)	Damping	Overshoot (%)	Frequency (radian)
Electromechanical mode	$-1.45 \pm 9.60i$	0.149	62.3	9.72
Exciter mode	$-5.90 \pm 9.59i$	0.469	18.9	10.90

With PID PSS	Position (rad/s)	Damping	Overshoot (%)	Frequency (radian)
Electromechanical mode	$-2.86 \pm 8.11i$	0.333	33.0	8.60
Exciter mode	$-3.47 \pm 11.00i$	0.301	37.1	11.50

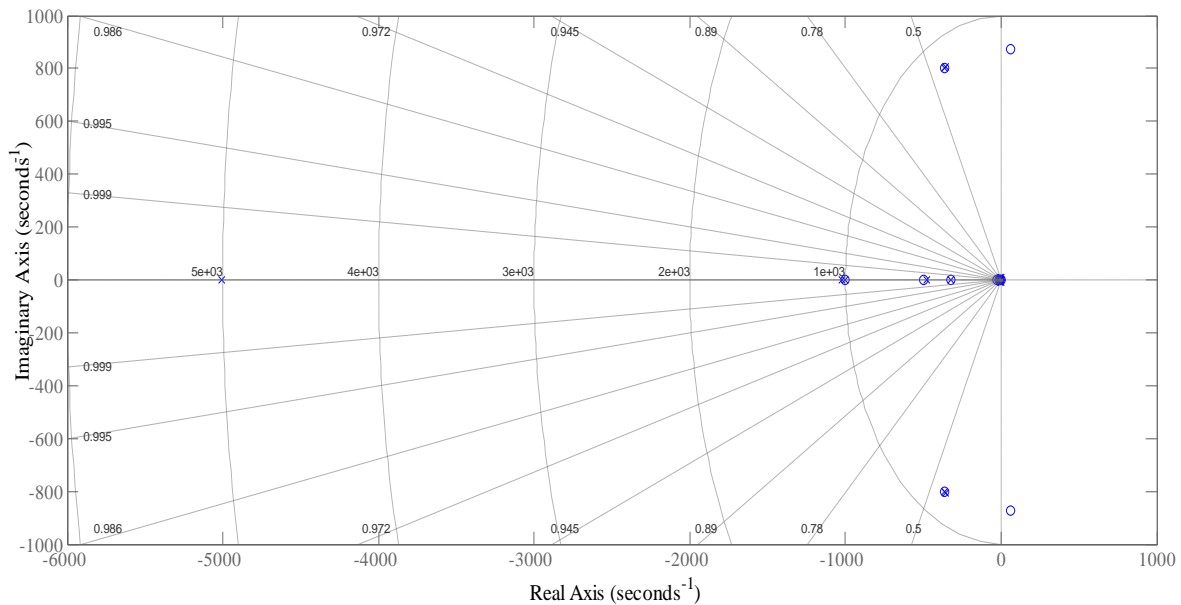


Fig. 6. Pole-Zero Map of the studied system without PID PSS.

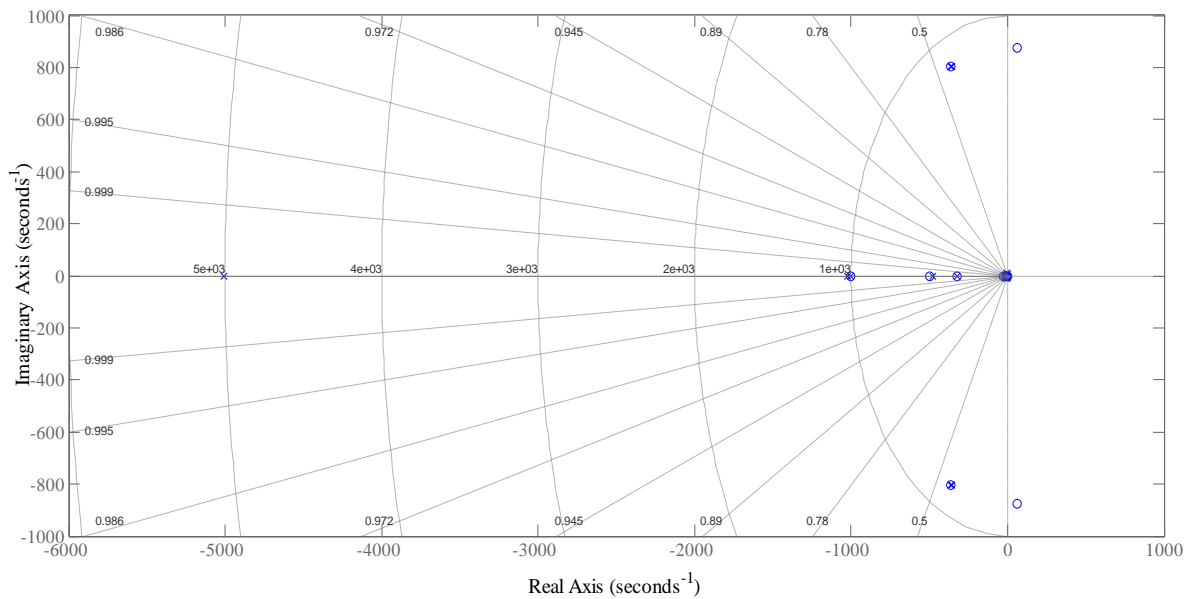


Fig. 7. Pole-Zero Map of the studied system with PID PSS.

IV. SIMULATION OF 50-MWE SOTEC PLANT

In this section we examine dynamic responses of the grid-connected SOTEC system under disturbance conditions in two separate subsections: first, we assess the impact of slow rate solar radiation on the quantities of our system. Next, we examine effectiveness of the designed PID PSS on the damping of system oscillations under severe three-phase short-circuit fault.

A. Slow Variation in Solar Radiation

System's response to variations of radiation are indicated below. In this section, using radiation data obtained from a meteorological station [18], we simulate the impact of solar radiation on our system. The data obtained from solar radiations are shown in Fig 9. We used Matlab software to process this data.

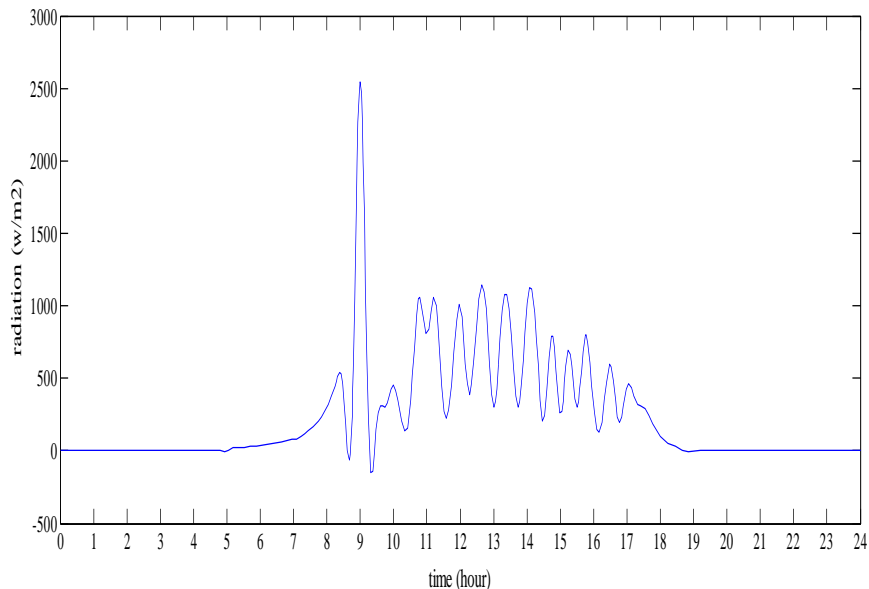


Fig. 8. Data related to measure solar radiations.

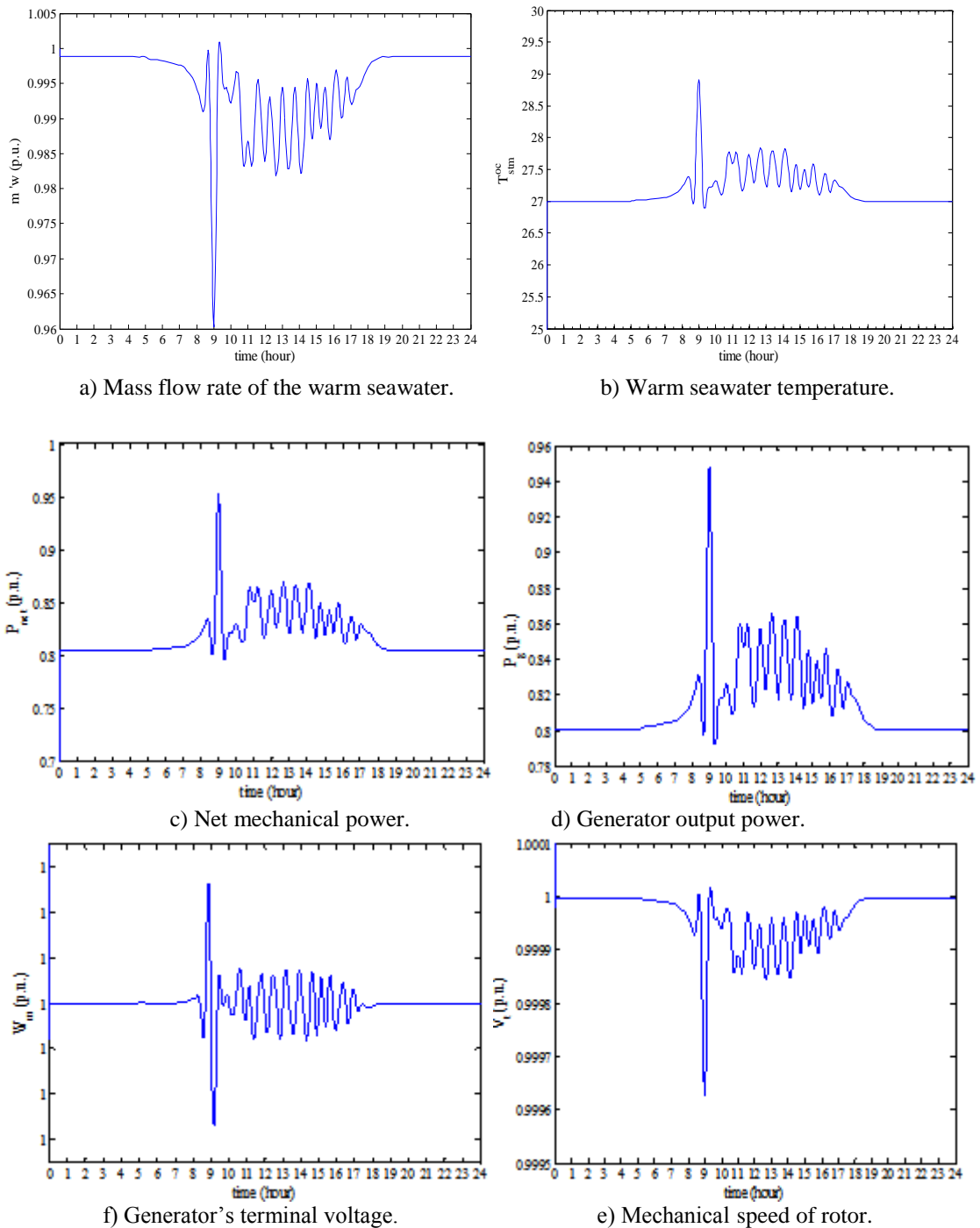


Fig. 9. Responses of the studied grid-connected SC-OTEC system under the slow variations of solar radiation.

Since changes in solar radiation are so slow, terminal voltage variation and rotor speed deviation have remained constant because of the effect of excitation system and turbine-governor. Variation in the temperature of water is associated to variation in solar radiation. However, there is deviation in it because of the impact of control system in order to mitigate such disturbance effect on mechanical power. Also, variations in pure mechanical power are associated with variations in warm water. Since PID PSS designed can work only in disturbance conditions, it cannot play a role in determining damping characteristics of system in long term variation in solar radiation.

B. Three Phase Short Circuit in Power Grid

Fig. 10. indicates transient responses from a grid-connected SOTEC system with and without the designed PID PSS under three-phase short-circuit fault in power grid. Fault occurs within 5 seconds from the beginning and lasts for 0.15 seconds. As it can be seen, there is an impact on damping in all functions of the system except voltage (because of the reduction in damping in exciter mode). Although this PSS has been linearized based on a linearized system model at a specified operating point using modal control theory without considering faulted conditions, but it is capable of providing appropriate damping conditions in order to decrease system oscillation under a three-phase short-circuit fault.

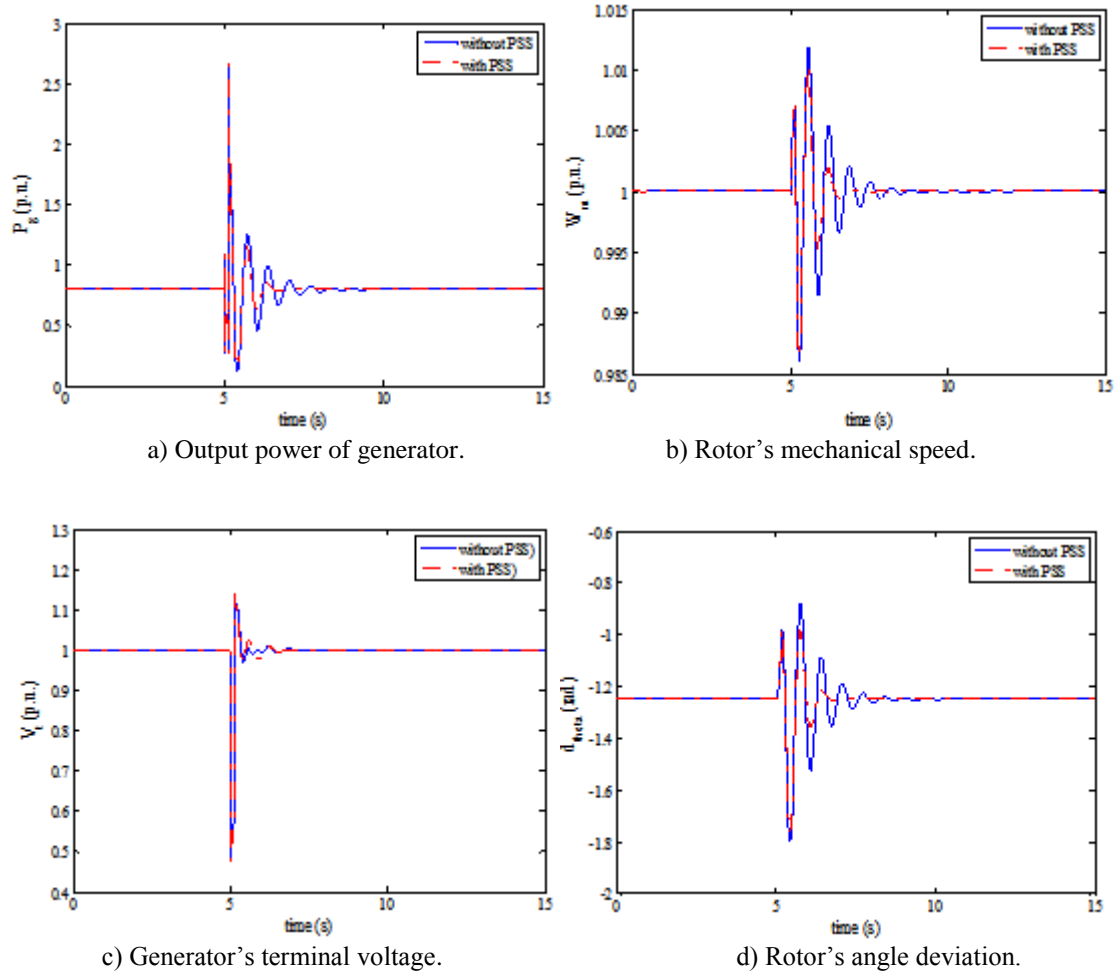


Fig. 10. System's transient response to a three-phase short-circuit fault at power grid.

V. CONCLUSION

In this paper we have examined the performance of a combined ocean thermal energy and solar thermal energy (SOTEC) system. Dynamic simulation results under disturbance conditions, slow variations in solar radiation, and severe short-circuit fault indicates that the system can function successfully. Also, we demonstrated the effects of appropriate designing of a stabilizer in a power system on increasing system stability and improvement of oscillations damping. Accordingly, we can claim that this proposed system can enhance the thermal efficiency of an OTEC plant, particularly in daytime operation.

APPENDIX

a) SC-OTEC system parameters [19]

Ocean surface temperature: 26 °c (Annual average)

Ocean temperature at 1000 m depth: 4.5 °c (Annual average)

Seawater flow rates: 264.6 m³/s (270,400 kg/s) of warm water; and, 138.6 m³/s (142,300 kg/s) of cold water

Cold seawater pipe inside diameter: 8.7 m

Aperture area of the parabolic mirror: 2200 m²

Absorptance of the absorber pipe: 0.9

Transmittance of the glass cover: 0.9

Heat loss coefficient for collector: 6 W/m² °c

Ambient temperature: 25°C
Water mass flow rate of SC: 5kg/s
Heat capacity of water: 4190.0J/kg °C
Collector efficiency factor: 0.841
Heat loss coefficient for collector of the heat exchanger: 3W/m² °C
Surface area of the heat exchanger: 10668.3m².

b) Synchronous generator

Nominal power, line-to-line voltage and frequency [P_n (MVA), V_n (KV_{rms}), f_n (Hz)]: [100, 13.8, 60]
Stator [R_s , L_l , L_{md} , L_{mq}] (pu): [0.00285, 0.114, 1.19, 0.36]
Field [R_f , L_{fd}] (pu): [0.000579, 0.114]
Dampers [R_{kd} , L_{kd} , R_{kq1} , and L_{kq1}] (pu): [0.0117, 0.182, 0.0197, and 0.384]
Inertia coefficient, friction factor, pole pairs [H(s), F (pu), p ()]: [3.7, 0, 20].

c) Transmission line and Submarine Power Cable

Line1:
Resistance per unit length (Ohms/km): 0.0529
Inductance per unit length (H/km): 0.0014
Capacitance per unit length (nF/km): 8.7749
Line length (km): 220
Line2:
Submarine Cable Length: 10km
Cable apparent resistance (Ohms/km): 0.102
Cable reactance (Ohms/km): 0.13
Cable capacitance (mF/km): 0.25.

d) Local load

$P_L = 10$ MW, $Q_L = 5$ MVar.

e) Transformer

Nominal power and frequency [P_n (MVA), f_n (Hz)]: [100, 60]
Winding 1 parameters [V_{1Ph-Ph} (V_{rms}), R_1 (pu), L_1 (pu)]: [13.8, 10⁻⁶, 0]
Winding 2 parameters [V_{2Ph-Ph} (V_{rms}), R_2 (pu), L_2 (pu)]: [230, 10⁻⁶, 0.15].

f) Steam turbine and governor

$K=20$, $T_1=0.001$ s, $T_2=0$ s, $T_3=0.1$ s, $T_{CH}=1.0$ s.

g) Excitation system

Low-pass filter time constant T_f (s): 0.02
Regulator gain and time constant [$K_a()$, T_a (s)]: [300, 0.001]
Exciter [$K_e()$, T_e (s)]: [1, 0]
Damping filter gain and time constant [$K_f()$, T_f (s)]: [0.001, 0.1]
Regulator output limits and gain [$E_{fmin}()$, E_{fmax} (pu), K_p ()]: [-11.5, 11.5, 0].

REFERENCES

- [1] Zener, Solar Sea Power, *Bulletin of the Atomic Scientists*, 35, 1976.
- [2] O. Bai, M. Nakamura, Y. Ikegami, and H. Uehara, "Simulation and evaluation of transient performance of ocean thermal energy conversion plant with working fluid of binary mixtures," in *Proc. Twelfth Int. Offshore and Polar Engineering Conf., Kitakyushu, Japan, May 2002*, pp. 641–648.
- [3] R. H. Yeh, T. Z. Su, and M. S. Yang, "Maximum output of an OTEC power plant," *Ocean Eng. J.*, vol. 32, no. 5, pp. 685–700, Apr. 2005.
- [4] P. J. T. Straatman and W. G. J. H. M. Sark, "A new hybrid ocean thermal energy conversion-offshore solar pond (OTEC-OSP) design: A cost optimization approach," *Solar Energy J.*, vol. 82, no. 6, pp. 520–527, Jun. 2008.
- [5] James F. George, *System Design Considerations for a Floating OTEC Modular Experiment Platform*, In *Proceedings of the 6th Ocean Energy Conference, volume 1*, 1979. Johns Hopkins University Applied Laboratory.
- [6] Noboru Yamada, Akira Hoshi, and Yasuyuki Ikegami, "Performance simulation of solar-boosted ocean thermal energy conversion Plant," *Renewable Energy* 34 (2009) 1752–1758
- [7] Li Wang, and Chen-Bin Huang, "Dynamic Stability Analysis of a Grid-Connected Solar-Concentrated Ocean Thermal Energy Conversion System", *IEEE TRANSACTIONS ON SUSTAINABLE ENERGY, VOL. 1, NO. 1, APRIL 2010*.
- [8] Amit Bhatia, Shreya Agarwal, and SwaminiKhurana, "Optimal Use of Waste Heat of Condenser of Thermal Power Plant," 978-1-4244-5586-7/10, 2010 IEEE.
- [9] Hyeon-Ju Kim, Ho-Saeng Lee, Seung-Won Lee, Dong-Ho Jung and Duck-Su Moon, "Mitigation of Environmental Impact of Power-plant Discharge by Use of Ocean Thermal Energy Conversion System," 978-1-4244-5222-4/10/ 2010 IEEE.

- [10] Ho-Saeng Lee, Young Kwon Jung, et al., "Manufacturing and Testing Mock-up for Commercialization of the Ocean Thermal Energy Conversion (50MW) Power Plant," 2011 IEEE.
- [11] H. P. Garg and R. K. Agarwal, "Some aspects of a PV/T collector/forced circulation flat plate solar water heater with solar cells," *Energy Convers. Manage. J.*, vol. 36, no. 2, pp. 87–99, Feb. 1995.
- [12] John Nagurny, Laura Martel et al., "Modeling Global Ocean Thermal Energy Resources", 0-933957-39-8, 2011 MTS.
- [13] G. C. Nihous, "An order-of-magnitude estimate of ocean thermal energy conversion resources," *ASME J. Energy Resources Technol.*, vol. 127, pp. 328–333, Dec. 2005.
- [14] IEEE Committee Report, "Dynamic models for steam and hydro turbines in power system studies," *IEEE Trans. Power App. Syst.*, vol. PAS-92, no. 6, pp. 1904–1915, Nov. 1973.
- [15] P. C. Krause, *Analysis of Electric Machinery* (New York: McGraw Hill, 1987).
- [16] P. Kundur, *Power System Stability and Control*, (New York: McGraw Hill, 1994) Ch. 8–9.
- [17] L. Wang, "A comparative study of damping schemes on damping generator oscillations," *IEEE Trans. Power Syst.*, vol. 8, no. 2, pp. 613–619, May 1993.
- [18] Hong Kong Observatory—the Government of the Hong Kong Special Administrative Region Jun. 19, 2008 [Online]. Available: <http://www.weather.gov.hk/>
- [19] Luis A. Vega, "First Generation 50 MW OTEC Plantship for the Production of Electricity and Desalinated Water", *Offshore Technology Conference* held in Houston, Texas, USA, 3–6 May 2010.